Archimer
http://archimer.ifremer.fr

Advances in measuring ocean salinity with an optical sensor

M Le Menn[1, *], J L de Bougrenet de la Tocnaye[2], P Grosso[2], L Delauney[3], C Podeur[3], P Brault[4]
and O Guillerme[4]

[1] Service Hydrographique et Océanographique de la Marine (SHOM), 13 rue du Chatellier, CS 92803, 29228 Brest Cédex 2, France
[2] TELECOM Bretagne, Technopôle de Brest-Iroise, CS 83818, 29238 Brest Cédex 3, France
[3] IFREMER, 155 rue Jean-Jacques Rousseau, 92138 Issy les Moulineaux Cédex, France
[4] NKE, Z.I. de Kerandré, 56700 Hennebont, France

*: Corresponding author : Marc Le Menn, email address : marc.lemenn@shom.fr

Abstract :

Absolute salinity measurement of seawater has become a key issue in thermodynamic models of the oceans. One of the most direct ways is to measure the seawater refractive index which is related to density and can therefore be related to the absolute salinity. Recent advances in high resolution position sensitive devices enable us to take advantage of small beam deviation measurements using refractometers. This paper assesses the advantages of such technology with respect to the current state-of-the-art technology. In particular, we present the resolution dependence on refractive index variations and derive the limits of such a solution for designing seawater sensors well suited for coastal and deep-sea applications. Particular attention has been paid to investigate the impact of environmental parameters, such as temperature and pressure, on an optical sensor, and ways to mitigate or compensate them have been suggested here. The sensor has been successfully tested in a pressure tank and in open oceans 2000 m deep.

Keywords : refractive index, seawater, density, salinity, refractometer

Glossary

A: incident angle (°)
A_i and B_i: coefficients of the Sellmeier relation
α_G et α_{Si}: expansion coefficient of glass and silicon (m-1)
C_1, C_2, C_3: constants
$d\lambda/dt$: Laser wavelength sensitivity to temperature (nm/°C)
dn: fluid refractive index variation
dn_{glass}/dp: pressure-optical coefficient (/dbar)
dn_{Glass}/dt: thermo-optical coefficient of glasses (/°C)
$\delta P(t, \lambda, p)$: correction to apply to the position P (μm)
dP: variation of the laser beam position (μm) corresponding to dn_{sea}
dr: variation of the refractive angle r (°)
δS^{Adens}: absolute salinity-density variation
ε: dielectric constant

ξ: proportionality constant

g_P: Gibbs function

i: refractive angle (°)

K: constant

λ: wavelength (nm)

L: length of the beam path (µm)

L_{max}: theoretical maximal length of the beam path (µm)

N: number of molecules per unit volume

n: fluid refractive index

n_L: refractive index of the left prism

n_R: refractive index of the right prism

m_p: molecular mean polarizability

m_r: molar refractivity

P: spot position on the PSD (µm)

p: pressure (dbar)

r: refractive angle (°)

ρ: density (kg/m^3)

σ: standard deviation

S_A: absolute salinity (g/kg)

S_A^{dens}: absolute salinity calculated from density measurements

S_p: practical salinity (no unit)

S_R: reference salinity (g/kg)

θ: half-angle between two prisms (°)

T: absolute temperature K)

t: temperature (°C)

W: molecular weight

1.Introduction

The recent re-definition of the Thermodynamic Equations Of Seawater[1] (TEOS-10), by the UNESCO/IOC SCOR/IAPSO working group 127 (WG127), based on a Gibbs potential function of Absolute salinity S_A, temperature T and pressure p, is questioning how to assess Absolute salinity. Nowadays, seawater salinity is calculated by formulas of the Practical Salinity Scale of 1978 (PSS-78)[2,3] based on conductivity ratio measured by conductance sensors. But, for seawater samples with different composition from standard seawater, Practical Salinity values S_p (which are dimensionless) present biaises[4].

First, they don't take into account non-ionic compounds dissolved in seawater causing deviations between S_A and S_p, S_A being the mass fraction of dissolved material in a given seawater sample, measured in standard conditions. S_A (expressed in g/kg) is directly related to the density ρ, a fundamental quantity in oceanography, and in order to take into account the problems related to the traceability to the International System of Units (SI), the WG127 has

defined the notion of 'Density Salinity' $S_A{}^{dens}$ which is the mass fraction of solution which has the same density as the sample it comes from, in standard temperature and pressure conditions. Then, models have been built to correct differences between S_A and S_p, and in 2009 McDougall *et al.*[4] have proposed to use the relation $S_A = S_R + \xi\delta S_A{}^{dens}$, where S_R is a Reference Salinity calculated from Practical Salinity measurement, ξ a proportionality constant and $\delta S_A{}^{dens}$ an empirical value obtained from a salinity value calculated from direct density measurements using the relation $\rho = 1/g_P(S_R, t, p)$, where g_P is the Gibbs function[5]. McDougall *et al.*[4] have assess the value of $\delta S_A{}^{dens}$ to be as large as 0.025 g/kg 'in the northernmost North Pacific' open ocean, mostly because of silicates which are non-ionic compounds. The assessment of this value is more delicate in coastal and estuarine waters.

Second, as showed by Setz *et al.*[6], the so-called IAPSO/standard seawater used to calibrate laboratory salinometers so that conductance sensors, and more precisely the reference salinity value, can be determined by this way only with a standard uncertainty of 0.01 with respect to the SI conductance standards, so that oceanographers community expects uncertainty values close to 0.002. According to Setz, it means that long timescale traceability of salinity measurements can be done only with a relative standard uncertainty of 3×10^{-4}, too large for oceanographic purposes. Furthermore, the uncertainty of $\xi\delta S_A{}^{dens}$ is difficult to estimate with respect to the SI, leading to SI-incompatible estimates of S_A[7]. Finally, conductivity depends strongly on temperature. That leads difficulties to align response times of conductance and temperature sensors. Because of S_p calculation with the PSS-78 relations, misalignments lead artefacts in salinity values, especially when measurements are made in non-mixed thermoclines. Even when data are corrected by the correction algorithms of instruments manufacturers, errors as large as 0.017 (on average) persist for measurements in strong salinity gradients[8]. That increases as much the uncertainty on practical salinity values.

To avoid these biases, measurements of the seawater refraction index are of particular interest. In 2009, we developed a method using advances in high resolution position sensitive devices (PSD), and taking advantage of small beam deviation measurements by a twin-prism refractometer[9]. This method has been employed to build a prototype, usable at sea to 2500 m in depth. In its development, special attention has been paid to the impact of environmental parameters, such as temperature and pressure on the optical sensor or temperature wavelength drift of the Laser, and ways have been settled to mitigate or compensate them. Salinity calculation and environmental variables compensation has been possible only by integrating in the instrument, sensors to measure external temperature and pressure and Laser internal

temperature. This prototype has been tested successfully, in a pressure tank and at sea to a 2000 m depth during an oceanographic cruise, and we have obtained the first deep sea index profile, calibrated in salinity.

2. Refractive index and density measurements theoretical background

It is well-known that density and absolute salinity can be assessed by a direct measurement of the refractive index. Different relations have been established to express refractive properties of fluids as a function of their state parameters[10]: $n^2-1 = K\rho$ found by Newton and Laplace (1821), $n-1 = K\rho$ found by Gladstone and Dale (1863), $(n^2-1)/(n + 0.4) = K\rho$ found by Eykman (1895) and,

$$\frac{\left(n^2 - 1\right)}{\left(n^2 + 2\right)} = K\rho \qquad (1)$$

found independently by Lorentz and Lorenz, in the same year (1880), where K is a constant. The Lorentz-Lorenz formula is the only one justified theoretically[11] and its second member is generally expressed in terms of molecular mean polarizability m_p and number of molecules per unit volume N. Relation (1) can then be written:

$$m_p = \frac{3}{4\pi N} \frac{\left(\varepsilon - 1\right)}{\left(\varepsilon + 2\right)} \qquad (2)$$

ε being the dielectric constant. If the molecular weight W of the species present in the fluid is known (it is the case for reference seawater[12]), the Lorentz-Lorenz relation can be expressed in terms of molar refractivity m_r, and relations (1) and (2) give:

$$\frac{\left(n^2 - 1\right)}{\left(n^2 + 2\right)} = \frac{m_r \rho}{W} \qquad (3)$$

For pure water, according to Reisler and Eisenberg, this equation does not describe correctly the observed shift between the temperature of the maximal refractive index and the temperature of the maximal density. They proposed in 1965 a semi-empirical relation describing the variations of the water refraction index[13]:

$$\frac{\left(n^2 - 1\right)}{\left(n^2 + 2\right)} = C_1 \rho^{C_2} e^{-C_3 t} \qquad (4)$$

In relation (4), C_1, C_2 and C_3 are constants depending on the wavelength λ. In 1984, Saubade showed that even in the case of water, the Gladstone-Dale refringence formula combined with the Reisler-Eisenberg relation gives the best results and can be generalised to any kind of liquid[14]. But, in the earlier formulation, Thormählen *et al*. verified the assumption that, if the Lorentz-Lorenz relation depends strongly on the wavelength, it varies slowly with temperature (no more than 1 % between ambient temperature and boiling point) and molar density[15]. Hence the molar refractivity of pure water behaves in the same way that other elementary fluid, for a given wavelength. This can be explained theoretically and modelled by an empirical relation function of ρ, t and λ [16].

On another way, several authors attempted to establish empirical relations between the seawater refractive index and its variations in temperature, salinity and pressure. In 1990, Millard and Seaver proposed a 27-terms algorithm covering the range 500 - 700 nm in wavelength, 0 - 30 °C in temperature, 0 - 40 in practical salinity and 0 - 11000 dbar in pressure, to compute the seawater refractive index[17]. By measuring the refractive index and inverting this algorithm, salinity can be extracted with accuracies close to oceanographic purposes at low pressure, but not at high pressure. This algorithm establishes a link between practical salinity and refractive index but, more recently, Millero and Huang have published relations between S_A and ρ, usable in the ranges of salinity 5 - 70 g kg^{-1} and temperature 273.15 to 363.15 K, with a standard error of 0.0036 kg m^{-3} in density, compatible with oceanographic purposes. Such relations are not usable with pressure values, but at this time, density can be computed as a function of practical salinity and pressure using Millero *et al*. equation[18]. This equation has been recently improved by measurements on standard seawater corresponding to S_A = 35.16504 g/kg, and extended temperature and pressure ranges[19], making density a good candidate for salinity traceability to SI[7], and refractometry for in-depth measurements, well suited to expected oceanographic accuracy.

3. Theoretical principle of the refractometer

Optical technologies have been considered for a long time as irrelevant to perform salinity measurements in depth, in open oceans, due to the ocean medium constraints[20]. Reported developments of sensor prototypes never resulted in regular applications due to lack of stability or reliability under temperature and pressure. Recent advances in high resolution position sensitive device (PSD) measuring beam deviations have enabled (with a 12 mm

Hamamatsu S3932) a full exploitation of fine deviations achievable by refractometers according to WG 127 requirements (i.e. uncertainty on refractive index of 1 ppm at atmospheric pressure and 3 ppm at high pressure). Various optical implementations are possible but for salinity measurements, where the impact of environmental features is critical, a twin-prism refractometer (TPR)[9] has been preferred because providing an intrinsic index thermal compensation.

TPR beam deviations are directly derived from the Snell-Descartes refraction laws:

$$n_L \, sin(A) = n \, sin(i) \quad \text{and} \quad sin(r) = \frac{n}{n_R} \, sin(2\theta - i) \qquad (5)$$

n_L and n_R being the refractive index of the left and right prism. Hence the beam deviation dr can be easily expressed as a function of the sea index variation dn.

$$\frac{cos(r)}{sin(r)} dr = \frac{\sqrt{1 - \frac{n}{n_R} sin(2\theta - i)^2}}{\frac{n}{n_R} sin(2\theta - i)^2} dr = \left(1 + \frac{cos(2\theta - i) sin(i)}{sin(2\theta - i) cos(i)}\right) \frac{dn}{n} \qquad (6)$$

$$\frac{dn}{dr} = \frac{n_R \, cos(i)}{sin(2\theta)} \sqrt{1 - \left(\frac{n}{n_R} sin(2\theta - i)\right)^2} \qquad (7)$$

with $cos(i) = \sqrt{1 - \left(\frac{n_L}{n} sin(A)\right)^2}$ and $dr = tan^{-1}\left(\frac{dP}{L}\right) \qquad (8)$

From (7) and (8), the refractive index resolution dn is obtained as:

$$dn = \frac{n_R}{sin(2\theta)} \sqrt{1 - \left(\frac{n_L}{n} sin(A)\right)^2} \sqrt{1 - \left(\frac{n}{n_R} sin(2\theta - i)\right)^2} \, tan^{-1}\left(\frac{dP}{L}\right) \qquad (9)$$

Relation (9) exhibits the design parameters (L, A, θ, n_L, n_R), whom the laser wavelength λ should be added. Most of these parameters are depending themselves on environmental parameters (t, p). Theoretically, L can be adjusted according to the required resolution and, the main parameter impacting the refractive index resolution is the incidence angle A. Fig.2 shows this dependence for $\theta = \pi/4$, $dP/L = 1.7$ µrad ($dP = 0.1$ µm, $L = 60$ mm) and $n = 1.34$.

A good trade-off is to choose A between the minimum deviation (~ 40 °) and total reflection (~ 60 °). The minimum deviation requires long prisms to cover the PSD whereas near total reflection is impinged by beam vignetting as well as the presence of turbid zone, at the two prisms junction. Fig.2 shows that from $A = 50$ °, dn is better than 1 ppm. Illustration is given for $A = 55$ °. Even if the length L seems free, it is not the case in practice. It is better to reduce the thermal inertia of the optical block by limiting the glass volume.

Two main environmental parameters will impact the performance: pressure and temperature. The pressure impacts the glass refractive index with a coefficient $dn_{Glass}/dp = 4\times10^{-8}/dbar$[21]. If the pressure is known with an accuracy of 2 dbar, the added uncertainty on salinity is $<<10^{-3}$ g.kg^{-1}, and can be neglected. It is not the case for the temperature which impacts several parameters, among which the laser wavelength $d\lambda/dt$, the refractive indices of glasses dn_L/dt and $d(dn_R)/dt$, the optical path length dL/dt and the PSD length Ldr/dt. Before estimating the influence of temperature on wavelength and refractive indices, let us determine the maximum length (L_{max}), beyond which it is impossible to maintain the refractometer resolution without electronic correction.

Figure 3 shows the optical block and sensor expansions as a function of L. Due to the symmetry along the PSD axis, the calculation is performed on one half of the PSD and for positive value t-t_0. Calling respectively α_G and α_{Si} the expansion coefficients of glass (optics) and silicon (PSD), we obtain:

$$dP_G = dr_{max}\times\alpha_G\times L\times(t - t_0) \quad \text{and} \quad dP_{Si} = dr_{max}\times\alpha_{Si}\times L\times(t - t_0)$$

$$\text{then :} \qquad dP = (\alpha_G - \alpha_{Si}) \times dr_{max} \times L\times(t - t_0) \qquad (10)$$

It results that the laser beam positioning error on the PSD as a function of the length L, for a deflection angle dr_{max} corresponding to a refractive index variation of 0.01 ($A = 55°$), a temperature change $t - t_0 = 20°C$, $\alpha_G = 12.7\times10^{-6}$, $\alpha_{Si} = 2.6\times10^{-6}$ follows a linear variation. Therefore, maintaining a positioning accuracy close to the PSD resolution without off-line corrections, results in an optimum length (L_{max}). This enables us to deduce from (5) the refraction angle dr corresponding to a seawater refractive index change of ± 0.01 (compared to 1.34) and to determine the most suitable PSD. For instance, with a PSD resolution of 0.2 μm we obtain a length $L \approx 60$ mm, with: $dn = \pm 0.01$, $\theta = \pi/4$, $A = 55°$, $n = 1.34$, $n_L = 1.515090$ and $n_R = 1.486010$, dr which is equal to ± 19 mrad. To garantee this resolution, the

laser beam should cover the usable PSD part (with the smallest beam waist) according to the considered refractive index (or salinity) range. Three types of high-resolution PSD are available: 3 mm (0.1 µm), 6 mm (0.2 µm), 12 mm (0.3 µm). By subtracting the laser beam waist (~500µm), we obtain L_{3mm} = 65.8 mm, L_{6mm} = 144.7 mm and L_{12mm} = 302.6 mm. According the above consideration, the expansion effect can only be neglected with the 3 mm PSD, maintaining the maximum refractometer resolution.

To make the optics insensitive to temperature variations, twin prisms (two half-prisms equivalent to Schott N-BK7 and N-FK5) are used whose thermo-optical coefficients have the same value but opposite–signs. From 0 ° to 40 °C: $(dn_L/dt) = 1.7 \times 10^{-6}$ °C^{-1} and $(dn_R/dt) = -1.7 \times 10^{-6}$ °C^{-1}. The refractive index variation of both optical prisms results in a self compensated variation of beam angular deflection. However the latter causes a shift of the output beam on the PSD. This implies that this shift is compensated by a same shift of the PSD. A solution to make the sensor fully insensitive to the thermo-optical effect is a PSD set-up on a substrate, whom the differential expansion coefficient allows a PSD motion with same value. The laser beam shift due to dn_{Glass}/dt equals minus the expansion holder shift (x) due to $d_{lengthholder}/dt$. The last parameter to be considered is the laser wavelength dependence on temperature (0.2 nm/°C). Temperature changes will cause a wavelength drift itself causing a refractive index change. This drift can be compensated electronically using the Sellmeier relationship[22]:

$$n_{Glass}^2 = 1 + \frac{A_1 \lambda^2}{\lambda^2 - B_1} + \frac{A_2 \lambda^2}{\lambda^2 - B_2} + \frac{A_3 \lambda^2}{\lambda^2 - B_3} \qquad (11)$$

A_i and B_i coefficients are provided by the manufacturers (e.g. Schott). These data allow establishing equations to compensate the refractive indices n_L and n_R with a good standard deviation ($\sigma = 4 \times 10^{-8}$):

$$n_L = 3 \times 10^{-9} t^2 - 5.21 \times 10^{-6} t + 1.5151172 \text{ and } n_R = 2 \times 10^{-9} t^2 - 7.666 \times 10^{-6} t + 1.4860987 \qquad (12)$$

For a given temperature and given wavelength, computed refractive indices are introduced into (9) to obtain dn. Another option consists in controlling the Laser diode temperature. A self-compensation of $d\lambda/dt$ is however difficult and/or expensive. A solution reducing this dependence by a factor ten (0.02 nm/°C) consists in using a broadband diode coupled with an interference filter. A salinity uncertainty of a few 10^{-3} g/kg can be obtained,

over the full salinity range 0-42 g/kg, the refractive index varying from 1.3325 (distilled water at room temperature and atmospheric pressure) to 1.3458 (the most salted seawater with 0 °C and 250 bars). This uncertainty can be improved close to 10^{-3} g/kg, in the max deviation angle configuration. This value is even better for small salinity (Fig. 4). Values of 2.4×10^{-4} g/kg have been obtained (10 g/kg)[23], making it appropriate for deep sea measurements. The choice of angle *A* depends on the PSD available resolution and the considered salinity range resulting in dedicated configurations for deep sea or coastal applications. Optical sensors provide a direct access to the absolute salinity unlike conductivity sensors exhibiting intrinsic errors of about 0.16 g/kg on the absolute salinity in some oceanic areas. They require a temperature and pressure accuracy of 2.10^{-2} °C and 1 dbar to compute salinity (i.e. with an order of magnitude smaller than for conductivity sensors).

4. Development and integration of the NOSS prototype

The refractometer has been containerized in order to be usable on *in situ* environmental mediums used in oceanography like surface buoys, sea bottom observatories, profiling Provor floats, gliders and CTD (Conductivity, Temperature, Depth) profilers. Compactness, pressure, temperature inertia, and corrosion have been major concerns during the design. This prototype has been called NOSS for NKE Optical Salinity Sensor.

Then, unlike the prototype describes in [9], the beam way has been deviated by gold mirrors deposited on angles of the prisms specially sized to reflect the beam on the PSD (Fig. 5 a)). In this way, the Laser diode and the PSD are on the same side of the instrument, making integration in a container, easier (Fig. 5 a)). A thermistor calibrated with Steinhart-Hart relation to an uncertainty of ± 0.005 °C, has been used to measure the water temperature near the optical sensing area. This thermistor is protected of pressure and humidity effects by a stainless steel thin rod (Fig.5). The Laser temperature is measured by a second thermistor calibrated to an uncertainty of ± 0.01 °C, fixed near it, inside the electronic container. A pressure sensor has been integrated near the base of the two prisms. Its measurement range is 0 – 300 bar and its initial accuracy ± 0.05 %.

Specific mechanical design and materials has been used in order to optimize the optical cell mounting in order to obtain complete independence versus temperature variations and pressure. The NOSS container has been tested under pressure up to 350 bar to check its tightness. A specific electronic board has been designed to allow high frequency

measurements up to 24 Hz in order to be compatible with CTD profilers. Special care has been taken during electronic design in order to reduce as much as possible the power consumption and measurement noise. The electronic system measures laser position up to the PSD, laser temperature and *in situ* temperature and pressure, in order to compute in final high precision density and salinity. The NOSS sensor is powered by a 12 Volts supply and consumes less than 600 mW. It has been successfully tested in laboratory to evaluate adverse effects due to in situ fluorescence and turbidity.

5. Calibration and correction in temperature, wavelength and pressure of the prototype

In order to assess the characteristics of the index measurements, the sensor has been placed in a calibration bath filled with seawater (S_p = 34,812, *turbidity* = 0.7 NTU) and which thermal stability can be regulated to better than 0.001 °C peak to peak, during 20 minutes, between 0 °C and 35 °C. The sensor's noise has been measured at 10 °C, in the bath stirred and not stirred. Stirring is produced by a propeller which generates strong helicoids laminar ascendant movements of water. It appears that the two extreme conditions of measurements generate average shifts in the order of only 1.10^{-6} on the value of the index but the stirring generates standard deviations 4 or 5 times higher than the quiet water where the index standard deviation is also in the order or less than 1.10^{-6}. It is explained probably by the index micro-gradients generated by quick variations of temperature as the beam cross the measurement volume.

Despite the careful design of the sensor, the Laser spot position on the PSD is sensible to the temperature of the PSD, the pressure applied on the prisms and the wavelength variations due to the Laser temperature. So, it is necessary to apply corrections δP on the measured positions P, as follow:

$$\delta P(t, \lambda, p) = \frac{\partial P}{\partial n}\left[\frac{\partial n}{\partial t}\delta t + \frac{\partial n}{\partial \lambda}\delta \lambda + \frac{\partial n}{\partial p}\delta p\right] \quad (13)$$

$\partial n/\partial \lambda$, $\partial n/\partial t$ and $\partial n/\partial p$ are obtained by deriving with respect to λ, t or p, the four expressions of Millard & Seaver Algorithm[17]. Laser diode sensitivity to temperature variations requires a correction of wavelength values used to compute the refractive index. The laser sensitivity to

temperature has been measured: $d\lambda/dt = 0.1899$ nm/°C. However, $\partial n/\partial\lambda$ is not constant to the needed accuracy for salinity variations > 1 unit, and it is necessary to estimate the salinity value before computing the correction $\delta P(\lambda)$. $\partial P/\partial n$ can be obtained by computing relation (9) and approximating n, or by measurements during the calibration. $\partial P/\partial n$ is then approximated per segments, by calculating positions, index and temperatures differences between temperature levels generated stepwise between 0 °C and 30 °C, in order to determine also $\partial P/\partial t$. Salinity being constant to ± 0.001 and pressure variations being negligible during the measurements, it appears that the sensitivity $\partial P/\partial t$ can be corrected by a simple 2^{sd} order polynomial of this kind: $\delta P(t) = 0.110\text{x}(-0.0040919 - 2.837\text{x}10^{-4}t + 1.3\text{x}10^{-6}t^2)$ ($r^2 = 0.9998$).

Then, pressure effects on P have been studied in a pressure tank. The sensor has been placed in a container equipped with a bladder sensible to pressure and a CTD profiler (SBE 37, Sea Bird Electronics), in order to measure conductivity, temperature and pressure variations. The container has been filled with seawater ($S_p = 33.8$), placed in the pressure tank, and pressure levels have been applied from atmospheric pressure to 2500 dbar. It appeared that P variations v.s. pressure are very linear (fig. 6). As the temperature and the salinity of the container were not constant to less than 0.002 during the experiment, P values have had to be corrected before to calculate the sensitivity $\partial P/\partial p$. The pressure corrections take then a simple form: $\delta P(p) = 1.194\text{x}10^{-4} - 3.694\text{x}10^{-9}p$, which leads a maximal residual error of $9\text{x}10^{-7}$ on the index.

The sensor being compensated in temperature, pressure and wavelength, the PSD voltage expressed in positions, can be calibrated in index. Values measured during temperature compensation can be used for that. Refraction index reference values are calculated with Millard and Seaver algorithm[16]. For $p = 0$ dbar and $S = 35$, the standard uncertainty of this algorithm is given to be $4.7\text{x}10^{-6}$ and the computation gives a linear relation of this kind: $n = 0{,}011496\text{x}P + 1.335718$ ($r^2 = 0.9992$).

6. Results of trials at sea

Trials have been realised at sea in spring 2010, during an oceanographic campaign in the Bay of Biscay. A 2000 m depth profile has been realised in an area where density variations are mostly due to temperature variations. A first refraction index profile has been measured to the frequency of 5 sample/s and a down cast speed of 0.5 m/s. This profile has been expressed in

salinity by inverting Millard and Seaver algorithm. He is similar to the one obtained with a reference CTD profiler, Sea Bird Electronics, SBE 9[+], used to recover the index sensor data, in that small salinity variation details can be compared. A second profile has been realised, at the same down cast speed, in a coastal area where density variations are mostly due to salinity variations. One time again, the index sensor is able to see the small salinity variations visible on the CTD profile, which proves the ability of this kind of sensor to be used at see in regular applications.

7. Conclusion

In the way to assess absolute salinity and sea water density, the refraction index theoretical method exposed in 2009 by Malardé *et al.*[9], has been used to develop an instrument called NOSS. In order to improve the compactness without to loose the resolution capacities of the theoretical method, mirrors have been added to the prisms and the beam path has been modified. This design allowed holding the Laser and the PSD on the same level in the container.

This prototype has been tested in a calibration bath to obtain correction relations between the measured Laser spot position and the temperature and wavelength variations. It has been tested also in a pressure tank to study the effect of pressure on the position. These measurements have showed it was possible to correct this sensor in order to hold the required accuracy, on the refraction index, of 1 ppm at atmospheric pressure and 3 ppm under high pressure, which confirms the theoretical studies made previously.

First trials at sea have shown promising results but, future studies are still necessary to improve the reliability and the thermal inertia of the sensor and to find corrections to align the index measurement response time to the temperature sensor one's, in order to improve salinity accuracy in strong temperature gradients. Measurements at higher pressures must also be foreseen in a new design.

technical assistance, F. Colas for turbidity and fluorescence tests, C. Schaeffer for the embedded software and A. Bodolec for the hardware. This work was supported by the FUI under grant NOSS.

Author Contributions

J.L. de Bougrenet and M. Le Menn initiated this project, J.L. de Bougrenet and P. Grosso investigated optical configurations, P. Grosso tested the optical prototypes, M. Le Menn followed the index-density-salinity relationships and performed the trials in laboratory and at sea, L. Delauney performed laboratory tests for environmental adverse effects , C. Podeur designed the containerization of the sensor, P. Brault coordinated the NOSS project as oceanographic instrumentation expert, O. Guillerme designed and tested electronic prototypes.

References

1. IOC, SCOR and IAPSO, 'The International Thermodynamic Equation of Seawater 2010 (TEOS-2010): Calculation and Use of Thermodynamic Properties', Intergovernmental Oceanographic Commission, Manuals and Guides n° 56, UNESCO, 156 pp, 2010.

2. Perkin R. G., Lewis E. L., 'The Practical Salinity Scale 1978: Fitting the Data', *IEEE J. Oceanic Eng.*, OE-5, n° 1, 9-16, 1980.

3. UNESCO, 'Algorithm for computation of fundamental properties of seawater', *UNESCO technical papers in Marine Sciences*, 36, 36p, 1983.

4. McDougall T. J., Jackett D. R., Millero F. J., 'An algorithm for estimating Absolute Salinity in the global ocean', *Ocean Sci. Discuss.*, 6, 215-242, 2009.

5. Feistel R., 'A Gibbs function for seawater thermodynamics for – 6 et 80 °C and salinity up to 120 g/kg', *Deep-Sea Res.* I, 55, 1639-1671, 2008.

6. Seitz S., Spitzer Petra, Brown R. J. C., 'CCQM-P111 study on traceable determination of practical salinity and mass fraction of major seawater components', *Accred. Qual. Assur.*, 15, 9-17, 2010.

7. Seitz S., Feistel R., Wright D. G., Weinreben S., Spitzer P., de Bièvre P., 'Metrological traceability of oceanographic salinity measurement results', *Ocean Sci. Discuss.*, 7, 1303-1346, 2010.

8. Mensah V., Le Menn M., Morel Y., 'Thermal mass correction for the evaluation of salinity', *J. Atmos. Oceanic Technol.*, 26, No. 3, 665–672, 2009.

9. D. Malardé, ZY Wu, P. Grosso, J.-L. de Bougrenet de la Tocnaye, M. Le Menn, "High-resolution and compact refractometer for salinity measurements", *Meas. Sci. and Tech.*, vol. 20 015204, (2009).

10. Saubade Ch., 'Refringency laws and optical properties of water at various temperatures: I', *J. Phys. C: Solid State Phys.*, 17, 3493-3506, 1984.

11. Born and Wolf, 'Principles of Optics, Electromagnetic Theory of Propagation, Interference and Diffraction of light', 6$^{\text{ème}}$ Edition, *Cambridge University Press*.

12. Millero F. J., Feistel R., Wright D. G., McDougall T. J., 'The composition of Standard Seawater and the definition of Reference-Composition Salinity Scale', *Deep-Sea Res.*, I, 55, 50-72, 2008.

13. Reisler E., Eisenberg H., 'Refractive Indices and Piezo-optic Coefficients of Deuterium Oxide, Methanol and other Pure Liquids', *The J. of Chem. Physics*, 43, 11, 3875-3880, 1965.

14. Saubade Ch., 'Refringency laws and optical properties of water at various temperatures: II. Macroscopic approach', *J. Phys. C: Solid State Phys.*, 17, 3507-3517, 1984.

15. Schiebener P., Straub J., Levelt Sengers J. M. H., Gallagher J. S., 'Refractive Index of Water and Steam as Function of Wavelenght, Temperature and Density', *J. Phys. Chem. Ref. Data*, 19, 3, 677-717, 1990.

16. Harvey A. H., Gallagher J. S., Levelt Sengers J. M. H., 'Revised Formulation for the Refractive Index of Water and Steam as a Function of Wavelength, Temperature and Density', , *J. Phys. Chem. Ref. Data*, 27, 4, 761-774, 1998.

17. Millard R.C., Seaver G., 'An index of refraction algorithm for seawater over temperature, pressure, salinity, density and wavelength', *Deep-Sea Res.*, Vol. 37, 12, 1909-1926, 1990.

18. Millero F. J., Chen C. T., Bradshaw A., Schleicher K., 'A new high pressure equation of state for seawater', *Deep-Sea Res.*, 27A, 255-264, 1980.

19. Safarov J., Millero F., Feistel R., Heintz A., Hassel E., 'Thermodynamic properties of standard seawater: extension to high temperatures and pressures', *Ocean Sci.*, 5, 235-246, 2009.

20. SCOR/IAPSO Working Group 127 on Thermodynamics and Equation of state of Seawater, 'Refractive index of seawater', Meeting 6$^{\text{th}}$-11$^{\text{th}}$ May 2007, Italy.

21. K-H. Mahrt and C. Waldmann, "Field proven high speed micro optical density profiler sampling 1000 times per second with 10^{-6} precision" *OCEANS '88, Proceedings*, vol.2, pp. 497-504, 1988.

22. W. Sellmeier, "Zur Erklärung der abnormen Farbenfolge im Spectrum einiger Substanzen", *Annalen der Physik und Chemie* **219**, 272-282, 1871.

23. P. Grosso, M. Le Menn, J.-L. de Bougrenet de la Tocnaye, ZY Wu, D. Malardé, "Practical versus absolute salinity measurements, new advances in high performance seawater salinity sensors", *Deep-Sea Research I*, vol. 57, n°1, 151–156, 2010.
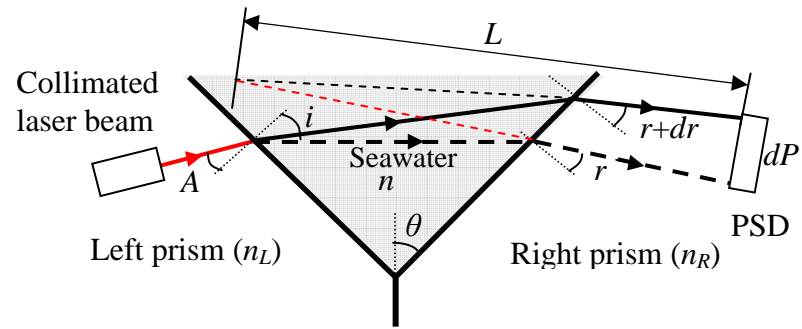
Figure 1: schematic diagram of twin-prism refractometer (TPR)
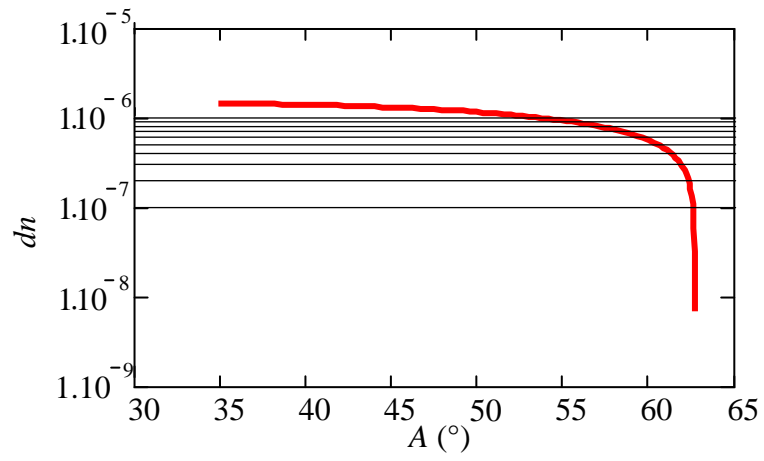
Figure 2: sensitivity of seawater refractive index to incident angle *A*.

PSD at $t > t_0$

PSD at t_0

Shift due to expansion of the prism (dP_V)

Shift due to expansion of the PSD (dP_{Si})

dr_{max} ($A = 55°$ and $dn = 0.01$)

PSD axis ($P = 0$, $n = 1.34$)

Prism length at t_0

Prism length at $t > t_0$

$t_0 = 0°C$

$0 < t < 40°C$
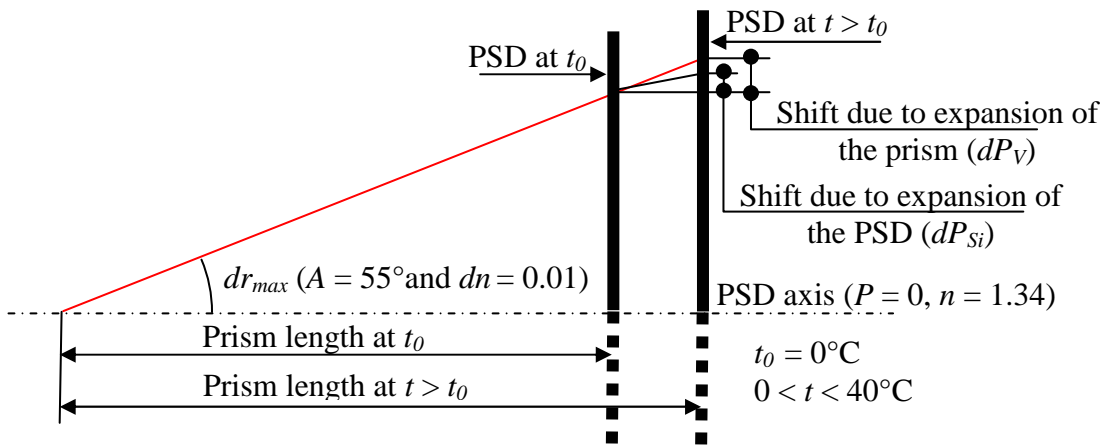
Figure 3: positioning error due to prism and PSD expansion
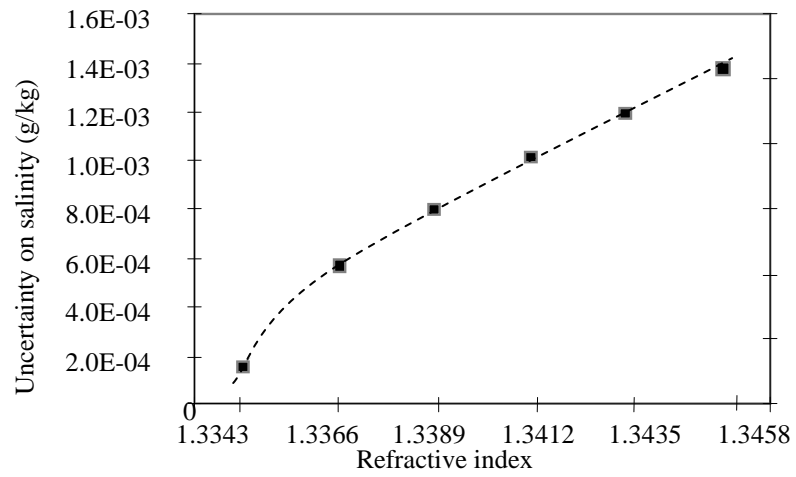
Figure 4: assessment from a theoretical functioning model of the uncertainty linked to the variation of the refractive angle on salinity measurements as a function of the medium refractive index. The refractive angle decreases when salinity increases.
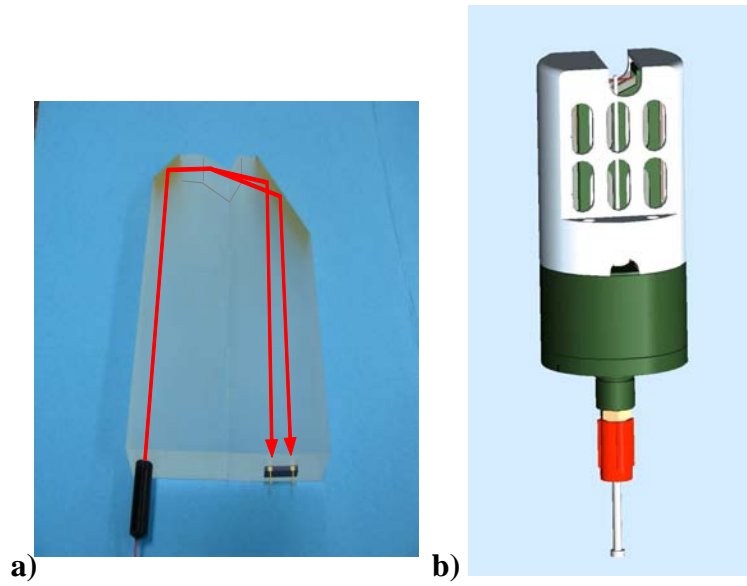
Figure 5: a) Optical part with the Laser on the left and the PSD on the right. The two beam paths correspond to the refractions obtained with seawater on the left and with distilled water on the right. **b)** NOSS sensor containerization. At the top part of the instrument, the measurement area is visible with the external temperature sensor contained in a long stainless steel rod. At the bottom part, there are the electronic container and the connector.
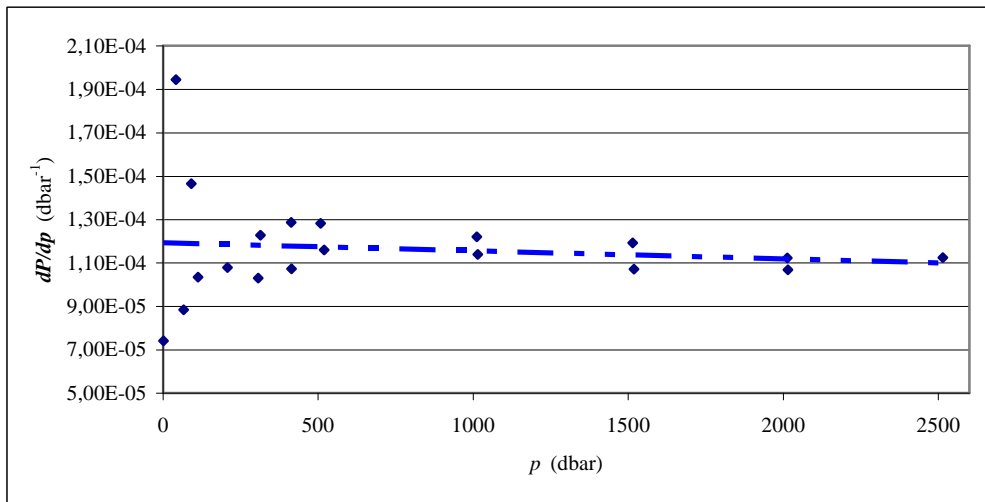
Figure 6: Dots represent the sensitivity of the PSD position (P) as function of the pressure (p) applied during the experiment in the pressure tank. The straight line (in blue) is the average correction applied to the data. Under 500 dbar, the positions data show an increasing discrepancy due to the inaccuracy of the corrections applied to the measured P. These corrections are necessary because the salinity decreased of 0.059 and the temperature of 1.508 °C during the measurements. But, by applying an average sensitivity $dP/dn = 81.431$ on the residual position errors, these discrepancies correspond only to maximal residual errors of 9×10^{-7} for increasing pressures and -5×10^{-7} for decreasing pressures, on the index.
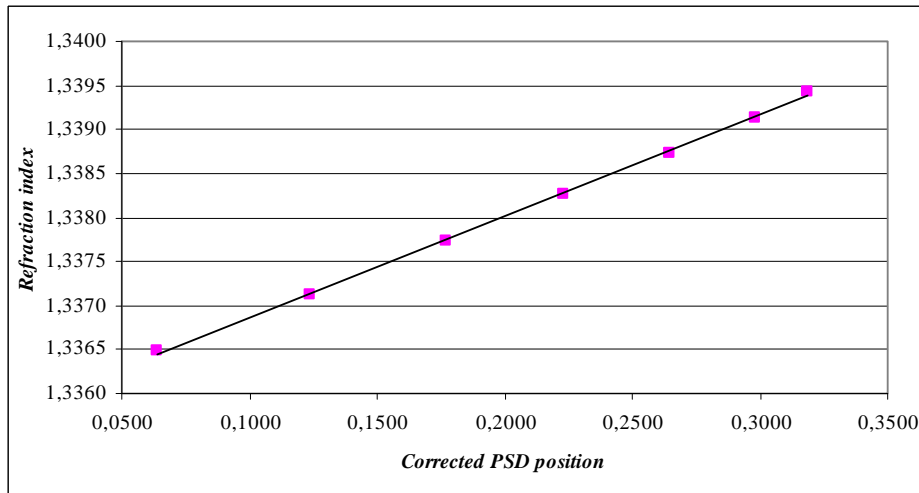
Figure 7: Result of the calibration of the corrected PSD positions as function of the refraction index. The relation is found to be very linear (Pearson correlation sampling coefficient $r^2 = 0.9992$).
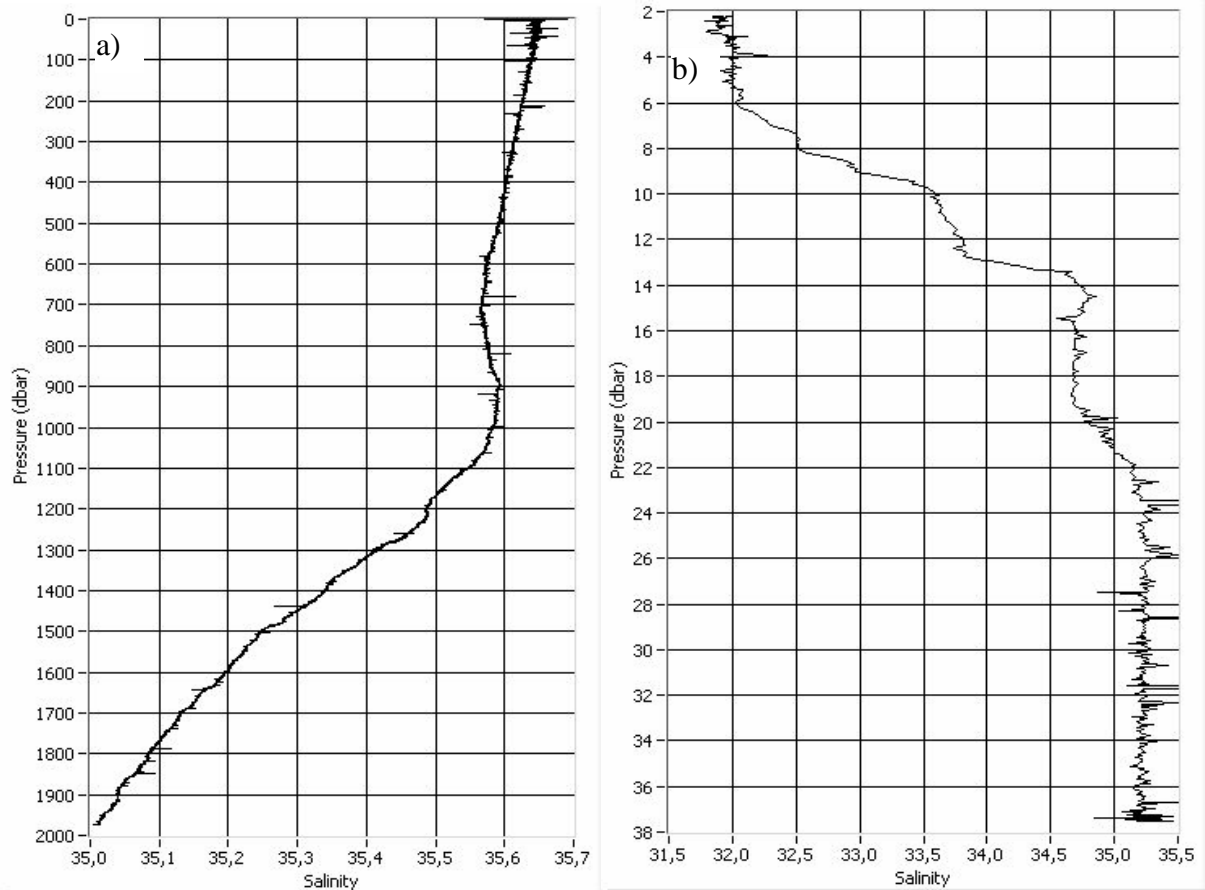
Figure 8: examples of index profiles obtained during an oceanographic campaign in the Bay of Biscay. Figure **a)** shows a 2000 m depth profile that has been realised in an area where density variations are mostly due to temperature variations. Acquired to the frequency of 5 sample/s, it has been expressed in salinity by inverting Millard and Seaver algorithm. Figure **b)** shows a profile obtained in a coastal area where density variations are mostly due to salinity variations. The two profiles are unfiltered and the response times of the index, temperature and pressure sensors have not been aligned, that can explain the visible spikes.